Coulomb Drag in Graphene Near the Dirac Point

M. Schütt,[1] P. M. Ostrovsky,[2,1,3] M. Titov,[4] I. V. Gornyi,[1,5] B. N. Narozhny,[6] and A. D. Mirlin[1,6,7]

[1]*Institut für Nanotechnologie, Karlsruhe Institute of Technology, 76021 Karlsruhe, Germany*
[2]*Max-Planck-Institut für Festkörperforschung, Heisenbergstrasse 1, 70569 Stuttgart, Germany*
[3]*L. D. Landau Institute for Theoretical Physics RAS, 119334 Moscow, Russia*
[4]*Radboud University Nijmegen, Institute for Molecules and Materials, NL-6525 AJ Nijmegen, The Netherlands*
[5]*A. F. Ioffe Physico-Technical Institute, 194021 Saint Petersburg, Russia*
[6]*Institut für Theorie der Kondensierten Materie and DFG Center for Functional Nanostructures, Karlsruher Institut für Technologie, 76128 Karlsruhe, Germany*
[7]*Petersburg Nuclear Physics Institute, 188350 Saint Petersburg, Russia*

(Received 22 May 2012; published 7 January 2013)

We study Coulomb drag in graphene near the Dirac point, focusing on the regime of interaction-dominated transport. We establish a novel, graphene-specific mechanism of Coulomb drag based on fast interlayer thermalization, inaccessible by standard perturbative approaches. Using the quantum kinetic equation framework, we derive a hydrodynamic description of transport in double-layer graphene in terms of electric and energy currents. In the clean limit the drag becomes temperature independent. In the presence of disorder the drag coefficient at the Dirac point remains nonzero due to higher-order scattering processes and interlayer disorder correlations. At low temperatures (diffusive regime) these contributions manifest themselves in the peak in the drag coefficient centered at the neutrality point with a magnitude that grows with lowering temperature.

DOI: 10.1103/PhysRevLett.110.026601 PACS numbers: 72.80.Vp, 73.23.Ad, 73.63.Bd

Frictional drag in double-layer systems consisting of two closely spaced, but electronically isolated conductors is a well established experimental tool for studying the microscopic structure of solids [1–7]. In such an experiment a current I_1 is passed through one of the conductors (the "active" layer) and the induced voltage drop V_2 is measured along the other ("passive") layer. The ratio of this voltage to the driving current $\rho_D = -V_2/I_1$ (known as the drag coefficient or the transresistivity) is a measure of both the interlayer interaction [1,2] and the microscopic state [3–6] of the layers. At low temperatures the drag effect is dominated by direct Coulomb interaction between the carriers in the two layers.

The physics of Coulomb drag is well understood if both layers are in the Fermi-liquid state [8,9], where the microscopic mechanism of the effect is based on the momentum transfer from the current-carrying state in the active layer to the passive layer by the interlayer Coulomb interaction. The interlayer momentum transfer can be described by the effective relaxation rate τ_D^{-1}. The most basic qualitative features of the drag measurement [1,8,9] can already be inferred by estimating τ_D^{-1} with the help of Fermi's golden rule, where it is crucial to take into account the energy dependence of the density of states (DOS) and/or diffusion coefficient D, reflecting the electron-hole (e-h) asymmetry.

The drag coefficient ρ_D and momentum relaxation rate τ_D^{-1} can be related using a simple Drude-like model. Consider the phenomenological equations of motion, assuming for simplicity that both layers are characterized by the same carrier density n and effective mass m

$$\frac{d}{dt}\begin{pmatrix}\boldsymbol{j}_1\\ \boldsymbol{j}_2\end{pmatrix} = \frac{e^2 n}{m}\begin{pmatrix}\boldsymbol{E}_1\\ \boldsymbol{E}_2\end{pmatrix} - \frac{1}{\tau_D}\begin{pmatrix}1 & -1\\ -1 & 1\end{pmatrix}\begin{pmatrix}\boldsymbol{j}_1\\ \boldsymbol{j}_2\end{pmatrix} - \frac{1}{\tau}\begin{pmatrix}\boldsymbol{j}_1\\ \boldsymbol{j}_2\end{pmatrix}, \tag{1}$$

where $\boldsymbol{j}_{1(2)}$ is the average current density in the active (passive) layer, $\boldsymbol{E}_{1(2)}$ is the electric field in the two layers, and τ is the impurity scattering time. Noting that in the drag measurement no net current is allowed to flow in the passive layer $\boldsymbol{j}_2 = 0$, we arrive at the Drude-like formula $\rho_D = -\rho_{12} = (e^2 n \tau_D/m)^{-1}$, where τ_D^{-1} may be estimated using Fermi's golden rule. More rigorous calculations based on either the diagrammatic perturbation theory [8] or the kinetic equation [9] result in the "Fermi-liquid" expression

$$\rho_D^{\mathrm{FL}} = (h/e^2) A_{12} T^2/(\mu_1 \mu_2), \tag{2}$$

where $\mu_{1(2)}$ is the chemical potential of the active (passive) layer and A_{12} is determined by the matrix elements of the interlayer interaction. (The precise form of A_{12} as a function of the interlayer spacing d depends on whether transport in the two layers is ballistic or diffusive [8].)

Even though the drag coefficient (2) is apparently independent of the impurity scattering time τ, transport properties of each individual layer are usually [1,8] assumed to be dominated by disorder, $\tau \ll \tau_D$: solving Eq. (1) for the resistivity one finds the usual Drude formula. In contrast, the behavior of clean double-layer systems, i.e., with $\tau \gg \tau_D$, is less trivial. In this case, the last term in Eq. (1) may be neglected leading to the nonzero result for the single-layer resistivity

$$\rho_{11} = -\rho_{12} = (e^2 n \tau_D/m)^{-1} = \rho_D. \quad (3)$$

Note, that the system is still characterized by the infinite conductivity ($\hat{\rho}^{-1} = \infty$), as expected for disorder-free conductors on the grounds of Galilean invariance.

The physical picture of the drag effect outlined so far is based on the following assumptions: (i) each of the layers is assumed to be in a Fermi-liquid state, which at the very least means $\mu_{1(2)} \gg T$; (ii) electron-electron interaction does not contribute to the transport scattering time; (iii) the interlayer Coulomb interaction is assumed to be weak enough, $\alpha = e^2/v_F \ll 1$ (we adopt the units where $\hbar = 1$ restoring the Planck's constant in final results), such that ρ_D is determined by the lowest-order perturbation theory [8].

Lifting one or more of the above assumptions leads to significant changes in the drag effect [3–5,7,10,11]. In this Letter we focus on the system of two parallel graphene sheets [7,10–21], which offers a great degree of control over the microscopic structure of the two layers. Indeed, using hexagonal boron nitride as a substrate [11,22], one can decrease disorder strength in the system and reach the regime, where transport properties of the two layers are dominated by electron-electron interaction, $\tau \gg \tau_{ee}$. Moreover, the carrier density can be electrostatically controlled allowing one to scan a wide range of chemical potentials from the Fermi-liquid regime to the Dirac point.

In this Letter we establish a drag mechanism based on fast interlayer thermalization in graphene (inaccessible by standard perturbative approaches to drag). Using the quantum kinetic equation (QKE) approach, we derive hydrodynamic equations generalizing Eq. (1) for interacting Dirac fermions (for related work in monolayer graphene see Refs. [23–25]). The distinct feature of the hydrodynamic approach to electronic transport in graphene is inequivalence of the electric current and total momentum. The latter is furthermore equivalent to the energy current. The resulting drag is governed by a nontrivial interplay of current and energy relaxation. In the ultraclean limit, this yields $\rho_D \sim (h/e^2)\alpha^2\mu_1\mu_2/(\mu_1^2 + \mu_2^2)$, which remains finite in the limit $\mu_1 = \mu_2 \to 0$. If disorder is present, then ρ_D is modified, see Figs. 1 and 2. At the Dirac point, the leading-order contribution to ρ_D vanishes due to e-h symmetry. Taking into account either the next-order ($\sim \alpha^3$) scattering or interlayer disorder, correlations yield a peak centered at the Dirac point with a magnitude that grows with lowering $T\tau$.

Kinetic equation.—We now briefly outline the derivation of the QKE for double-layer graphene structures and its solution in the ballistic regime (see Supplemental Material [26]). Consider an infinite sample in an infinitesimal, homogeneous electric field $\boldsymbol{E}_1$ applied to the active layer. The response of the system to the field can be described by the small nonequilibrium corrections $h_{1(2)}$ to the Fermi distribution functions defined by

$$n_i(\epsilon, \hat{\mathbf{v}}) = n_F^{(i)}(\epsilon) + T\frac{\partial n_F^{(i)}(\epsilon)}{\partial \epsilon} h_i(\epsilon, \hat{\mathbf{v}}), \quad (4)$$

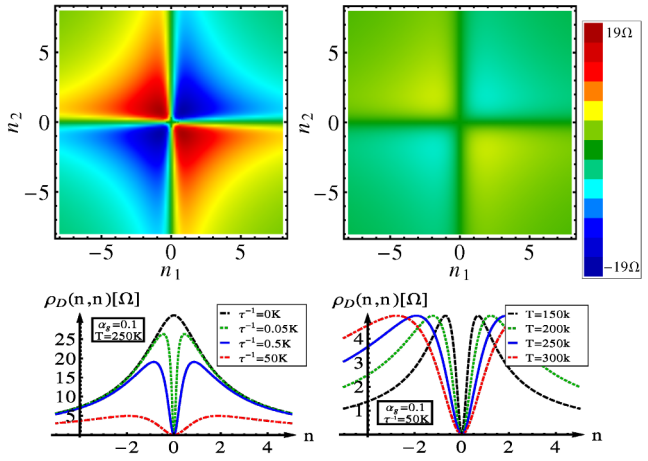

FIG. 1 (color online). Leading-order drag coefficient in the ballistic regime as a function of carrier densities (in units of 10^{11} cm^{-2}) for $d = 9$ nm. Left: ρ_D at $T = 250$ K; the upper left panel refers to ultraclean graphene $\tau^{-1} = 0.5$ K; the lower left panel shows the evolution of ρ_D with increasing disorder from $\tau^{-1} = 0$ to $\tau^{-1} = 50$ K. Right: ρ_D for $\tau^{-1} = 50$ K; the lower panel shows ρ_D for $T = 150$, 200, 250, and 300 K.

where the eigenstates of the Dirac Hamiltonian $H = v\boldsymbol{\sigma}\boldsymbol{p}$ are labeled [26] by their energy ϵ and the velocity unit vector $\hat{\mathbf{v}}$; the momentum of the particle is $\boldsymbol{p} = \epsilon\hat{\mathbf{v}}/v$.

Linearizing the QKE [27] for small h_i we find

$$\frac{\partial h_1}{\partial t} + \frac{e\boldsymbol{E}_1 \cdot \boldsymbol{v}}{T} = -\frac{h_1}{\tau} + I_{11}\{h_1\} + I_{12}\{h_1, h_2\},$$
$$\frac{\partial h_2}{\partial t} = -\frac{h_2}{\tau} + I_{22}\{h_2\} + I_{21}\{h_2, h_1\}, \quad (5)$$

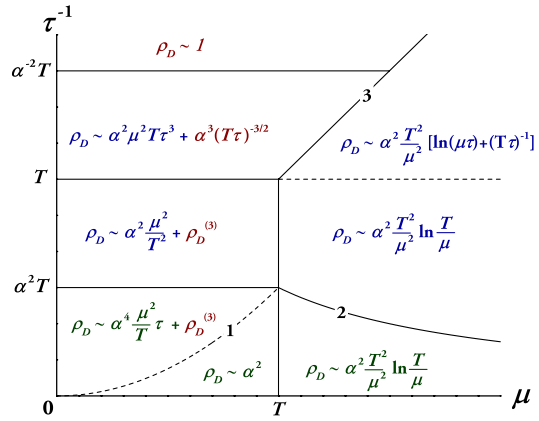

FIG. 2 (color online). Drag coefficient for identical layers, $\mu \ll \min(T/\alpha, v/d)$, and uncorrelated disorder. Bottom row ($\tau^{-1} \ll \alpha^2 T$ and below the curve 2, $\tau^{-1} \ll \alpha^2 T^2/\mu$): solutions of the QKE (12). Curve 1 ($\tau^{-1} = \alpha^2\mu^2/T$) separates the two regimes in Eq. (14). Middle row ($\alpha^2 T \ll \tau^{-1} \ll T$): region where the QKE approach overlaps with the perturbation theory of Ref. [16]. The third-order contribution $\rho_D^{(3)} = \mathcal{O}(\alpha^3)$ yielding nonzero drag at $\mu = 0$ is shown in red. Upper row ($\tau^{-1} \gg T$): diffusive regime [see Eqs. (16) and (17)], where $\rho_D^{(3)}$ saturates for $\tau^{-1} \gg T/\alpha^2$).

where the linearized pair-collision integrals are given by

$$I_{ij} = -\int d2d3d4W^{ij}(h_{i,1} - h_{i,2} + h_{j,3} - h_{j,4}),$$
$$W^{ij} = \delta(\boldsymbol{p}_1 - \boldsymbol{p}_2 + \boldsymbol{p}_3 - \boldsymbol{p}_4)\delta(\epsilon_1 - \epsilon_2 + \epsilon_3 - \epsilon_4) \times \frac{\cosh\frac{\epsilon_1-\mu_i}{2T}}{2\cosh\frac{\epsilon_2-\mu_i}{2T}\cosh\frac{\epsilon_3-\mu_j}{2T}\cosh\frac{\epsilon_4-\mu_j}{2T}} K^{ij}_{1,2;3,4}, \quad (6)$$

and we have used short-hand notations $h_{i,a} = h(\epsilon_a, \hat{\mathbf{v}}_a)$, $da = \nu(\epsilon_a)d\hat{\mathbf{v}}_a d\epsilon_a$, with $a = 1, 2, 3, 4$. To the lowest order in interlayer interaction, the kernel

$$K^{ij}_{1,2;3,4} = |U^{ij}(\boldsymbol{p}_1 - \boldsymbol{p}_2)|^2(1 + \hat{\mathbf{v}}_1\hat{\mathbf{v}}_2)(1 + \hat{\mathbf{v}}_3\hat{\mathbf{v}}_4)/4, \quad (7)$$

comprises the interaction matrix element $|U^{ij}|^2$ and the Dirac factors. Here we take into account only the Hartree interaction term: there is no exchange interaction between the layers, whereas within the layers the Hartree term dominates if the number of electron flavors is large (physically, $N = 4$ due to spin and valley degeneracy).

The peculiarity of the inelastic scattering in the Dirac spectrum is twofold. First, since the velocity $\boldsymbol{v} = v^2\boldsymbol{p}/\epsilon$ is independent of the absolute value of the momentum, total momentum conservation does not prevent velocity (or current) relaxation. As a result, the intralayer collision integral I_{ii} yields a nonzero transport relaxation rate due to electron-electron scattering.

Second, the scattering of particles with almost collinear momenta is enhanced since the momentum and energy conservation laws coincide for collinear scattering. This restricts the kinematics [23,24,28] of the Dirac fermions leading to the singularity in the collision integral. This singularity leads to the fast thermalization of particles within a given direction, which justifies the Ansatz:

$$h_i(\epsilon, \hat{\mathbf{v}}) = (\chi_v^{(i)} + \chi_p^{(i)}\epsilon/T)e\boldsymbol{E}\cdot\boldsymbol{v}/T^2. \quad (8)$$

The Ansatz (8) retains the only two relevant modes for which the collision integral I_{ij} is not singular: the "momentum mode" $\chi_p^{(i)}$, which nullifies the collision integral due to momentum conservation, and the "velocity mode" $\chi_v^{(i)}$, which nullifies I_{ij} in the case of collinear scattering. The same kinematic restrictions lead to fast unidirectional thermalization between the layers. This allows us to set $\chi_p^{(1)} = \chi_p^{(2)}$, and hence reduce the QKE for the double-layer setup to a 3×3 matrix equation.

Consider for simplicity the case of identical layers (for the more general case of $\mu_1 \neq \mu_2$ see Supplemental Material [26]). Integrating the reduced QKE over the energies, we arrive at the set of steady-state hydrodynamic equations in terms of the particle currents

$$\boldsymbol{J}_i = -NT\int d\epsilon\nu(\epsilon)\frac{\partial n_F^{(i)}}{\partial\epsilon}\int d\hat{\mathbf{v}}\boldsymbol{v}h_i(\epsilon, \hat{\mathbf{v}}), \quad (9)$$

and the total momentum $\boldsymbol{P} = e\epsilon_0 C_1^2(\boldsymbol{E}_1 + \boldsymbol{E}_2)\tau$:

$$e\epsilon_0\begin{pmatrix}\boldsymbol{E}_1\\ \boldsymbol{E}_2\end{pmatrix} = \left[\frac{1}{\tau} + \hat{I}_{ee} - \hat{I}_D\right]\begin{pmatrix}\boldsymbol{J}_1\\ \boldsymbol{J}_2\end{pmatrix} + \left[\frac{1}{\tau_D} - \frac{1}{\tau_{ee}}\right]\begin{pmatrix}\boldsymbol{P}\\ \boldsymbol{P}\end{pmatrix}, \quad (10)$$

where $\hat{I}_{ee(D)} = [(\hat{\sigma}_0 + \hat{\sigma}_1)C_1^2 + 2\hat{\sigma}_{0(1)}C_2]/\tau_{ee(D)}$. The intra- and interlayer electron-electron transport scattering rates are ($\mathcal{W}^{ij} = W^{ij}/\cosh^2[(\epsilon_1 - \mu_i)/(2T)]$)

$$\frac{1}{\tau_D} = \frac{1}{4T\epsilon_0 C_2}\int\prod_{a=1}^{4} da\,\mathcal{W}^{12}(\boldsymbol{v}_1 - \boldsymbol{v}_2)(\boldsymbol{v}_4 - \boldsymbol{v}_3),$$
$$\frac{1}{\tau_{ee}} = \frac{1}{8T\epsilon_0 C_2}\int\prod_{a=1}^{4} da[\mathcal{W}^{11}(\boldsymbol{v}_1 - \boldsymbol{v}_2 + \boldsymbol{v}_3 - \boldsymbol{v}_4)^2 + 2\mathcal{W}^{12}(\boldsymbol{v}_1 - \boldsymbol{v}_2)^2], \quad (11)$$

σ_k are the Pauli matrices in "layer space", the coefficients $C_1 = \langle\epsilon\rangle_\epsilon/T \sim \mu/T$, $C_2 = (\langle\epsilon^2\rangle_\epsilon - \langle\epsilon\rangle_\epsilon^2)/T^2 \sim$ const are the average energy and energy variation, $\epsilon_0 = 2T\mathcal{J}\{1\}/N$ is a typical energy, and

$$\mathcal{J}\{\cdots\} = -\frac{v^2}{T}\int d\epsilon\nu(\epsilon)\frac{\partial n_F}{\partial\epsilon}\cdots, \qquad \langle\cdots\rangle_\epsilon = \frac{\mathcal{J}\{\cdots\}}{\mathcal{J}\{1\}}.$$

The hydrodynamic equations (10) generalize the equations of motion (1) to the case of Dirac fermions. The kinematic peculiarity of Dirac fermions manifests itself in the appearance of the total momentum (energy current), which entangles the electric fields in the two layers. Solving Eq. (10) we find

$$\rho_D^{(2)} = \frac{h}{e^2}\frac{C_2}{2\pi\epsilon_0}\frac{(\tau\tau_D)^{-1} + C_1^2[\tau_{ee}^{-2} - \tau_D^{-2}]}{\tau^{-1} + C_1^2[\tau_{ee}^{-1} - \tau_D^{-1}]}. \quad (12)$$

Equation (12) gives the general expression for the drag coefficient in the ballistic regime (see Fig. 1 for illustration). Below, we discuss the asymptotic behavior of ρ_D (summarized in Fig. 2) focusing on the experimentally relevant case [7,10,11] $Td/v < 1$.

Clean system.—In the limit $\tau \to \infty$, the resistivity matrix is degenerate and the drag coefficient is given by

$$\rho_D^{(2)}(\tau \to \infty) = (h/e^2)(C_2/2\pi\epsilon_0)(\tau_D^{-1} + \tau_{ee}^{-1}). \quad (13)$$

This result illustrates the remarkable feature of double-layer graphene, where in addition to the standard drag mechanism due to direct interlayer current relaxation (τ_D^{-1}), there exists another mechanism governed by the interplay of fast interlayer energy relaxation ($\tau_E^{-1} \gg \tau_{ee}^{-1}$) and intralayer current relaxation (τ_{ee}^{-1}), which is insensitive to the e-h asymmetry.

At the Dirac point $\mu = 0$, Eq. (13) yields nonzero drag already in the lowest order in the interlayer interaction $\rho_D^{(2)} \sim (h/e^2)\alpha^2$ (where it is determined by $\tau_{ee}^{-1} \sim \alpha^2 T$; the "drag rate" τ_D^{-1} appears only in the next order, $\tau_D^{-1}(\mu = 0) \sim \alpha^3 T$ and remains subleading).

Ballistic regime.—For weak, uncorrelated disorder $\alpha^2 T\tau \gg 1$ (i.e., $\tau^{-1} \ll \tau_{ee}^{-1}$), the lowest-order contribution

to ρ_D near the Dirac point can be obtained from Eq. (12) by setting $\tau_D^{-1} \sim \alpha^2\mu_1\mu_2/T$, $\tau_{ee}^{-1} \sim \alpha^2 T$, $\epsilon_0 \sim T$, $C_1^2 \sim \mu_1\mu_2/T^2$, and $C_2 \sim 1$:

$$\rho_D^{(2)}(\mu_i \ll T) \approx 2.87\frac{h}{e^2}\alpha^2\frac{\mu_1\mu_2}{\mu_1^2+\mu_2^2+0.49T/(\alpha^2\tau)}. \quad (14)$$

Precisely at the Dirac point $\rho_D^{(2)}(\mu_i = 0) = 0$, while in the immediate vicinity ρ_D grows sharply, see Fig. 1. However, refining the collision integrals (6) by taking into account either (i) the next-order matrix elements, or (ii) interlayer disorder correlations, leads to non-zero $\rho_D(\mu_i = 0)$ [26]. In the former case we find $\rho_D^{(3)}(\mu_i = 0) \sim (h/e^2)\alpha^3$. The result in the latter case depends on the length scale characterizing the correlations: within the model of correlated impurity scattering $\rho_D^{\rm corr} \sim (h/e^2)\alpha^2/(T\tau)$; for long-range correlations we find $\rho_D^{\rm corr} \sim (h/e^2)\alpha^2 T^{-2} F_{12}^{(\mu)}(0)(1+\alpha^2 NT\tau)$, where $F_{12}^{(\mu)}(0)$ is the correlator of chemical potential fluctuations in the two layers [26,29].

For intermediate disorder strength $\alpha^2 T \ll \tau^{-1} \ll T$ the applicability region of the QKE overlaps with that of the conventional perturbation theory developed in Ref. [16] and we recover perturbative results, see Fig. 2.

Diffusive regime.—For even stronger disorder (or at low temperatures) $T\tau \ll 1$, the electron motion becomes diffusive. In this regime, the standard perturbative approach is applicable. The lowest-order perturbative calculation [8] amounts to evaluation of the Aslamasov-Larkin-type diagram for the drag conductivity given by

$$\sigma_D^{\alpha\beta} = \frac{1}{16\pi T}\sum_{\mathbf{q}}\int\frac{d\omega}{\sinh^2\frac{\omega}{2T}}\Gamma_1^\beta(\omega,\boldsymbol{q})\Gamma_2^\alpha(\omega,\boldsymbol{q})|\mathcal{D}_{12}^R|^2, \quad (15)$$

where $\mathcal{D}_{12}^R$ is the retarded propagator of the interlayer interaction and $\Gamma_a^\alpha(\omega,\boldsymbol{q})$ is the nonlinear susceptibility [in fact, all previous studies of the Coulomb drag in graphene [12–20] focused on Eq. (15)]. In the diffusive regime, $\Gamma_a^\alpha(\omega,\boldsymbol{q})$ can be found using Ohm's law and the continuity equation [30] $\boldsymbol{\Gamma} = e\boldsymbol{q}(\partial\sigma/\partial n)\mathrm{Im}\Pi^R$. Close to the Dirac point $\mu \ll T \ll \tau^{-1}$ the derivative $\partial\sigma/\partial n \sim n v^4\tau^4$ (independently of the precise nature of impurities). After this the evaluation of Eq. (15) is rather standard (except that, in contrast to Ref. [8], the Thomas-Fermi screening length is much longer than the interlayer spacing $\varkappa d \ll 1$) and yields

$$\rho_D^{(2)}(\mu_i \ll T \ll \tau^{-1}) \sim (h/e^2)\alpha^2\mu_1\mu_2 T\tau^3, \quad (16)$$

vanishing at $\mu_i = 0$ due to the electron-hole symmetry.

The importance of the electron-hole asymmetry for $\rho_D^{(2)}$ follows from Eq. (15): the nonlinear susceptibility can be thought of as a measure of the asymmetry. But $\rho_D^{(2)}$ dominates the observable effect only under standard assumptions of the Fermi-liquid behavior in the two layers ($\mu \gg v/d \gg T$, $\mu\tau \gg 1$). On the contrary, in the vicinity of the Dirac point in graphene, the next-order contribution

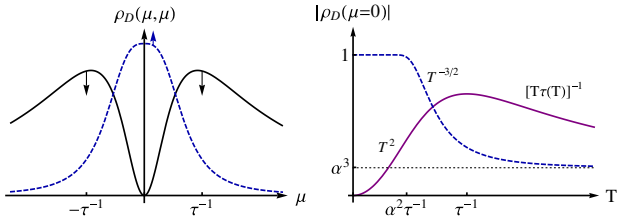

FIG. 3 (color online). Schematic view of the drag coefficient at low temperatures. Left: $\rho_D^{(2)}(\mu)$ (solid line) and $\rho_D^{(3)}(\mu)$ (blue dashed line). The arrows indicate the tendency of the two terms with the decrease of temperature $T \to 0$. Right: $\rho_D^{(3)}(\mu = 0)$ and $\rho_D^{\rm corr}(\mu = 0)$ (solid line) as functions of T [26].

$\rho_D^{(3)}$ [31] as well as disorder correlations [26,32] become important and yield non-zero drag at $\mu_i = 0$.

The explicit results of Ref. [31] were obtained in the usual limit $\varkappa d \gg 1$. Extending these calculations to the opposite case $\varkappa d \ll 1$ we find close to the Dirac point

$$\rho_D^{(3)}(\mu_i \ll T \ll \tau^{-1} \ll \alpha^{-2}T) \sim (h/e^2)\alpha^3(T\tau)^{-3/2}, \quad (17)$$

and $\rho_D^{(3)} \sim h/e^2$ for $\tau^{-1} \gg \alpha^{-2}T$ (at the same time $\rho_D^{\rm corr}$ vanishes at low T as $\rho_D^{\rm corr} \sim (h/e^2)\alpha^2(T\tau)^2$ [26]). Away from the Dirac point this contribution decays as a function of the chemical potential $\rho_D^{(3)}(\mu\tau \gg \max[1, \alpha^{-1}(T\tau)^{1/2}]) \sim (h/e^2)(\mu\tau)^{-3}$ and rapidly becomes subleading. As a result, $\rho_D^{(3)}$ is only detectable at low T and μ, see Fig. 3.

While estimating $\rho_D^{(3)}(\mu_i = 0)$, we assume the single-layer conductivity $\sigma \sim e^2/h$ discarding localization effects: experiments on high-quality samples show T-independent σ down to 30 mK [33], that can be explained by the specific character of disorder in graphene [34].

Summary.—We have studied Coulomb drag in double-layer graphene structures. We have shown that drag in graphene drastically differs from that in conventional double-layer structures. By using the QKE formalism, we have derived the hydrodynamic description and established a graphene-specific drag mechanism based on fast interlayer thermalization. For weak disorder (or high T; ballistic regime) ρ_D near the Dirac point is given by Eq. (14), see also Fig. 1, which is consistent with Ref. [10]. For strong disorder (or low T; diffusive regime), the usually subleading third-order and correlated disorder contributions dominate the effect and yield a peak centered at the Dirac point similar to experiment [11,35].

We thank A. K. Geim, K. S. Novoselov, and L. Ponomarenko for communicating their experimental results prior to publication. We are grateful to J. Schmalian, M. Müller, V. Kachorovskii, A. Dmitriev, D. Polyakov, and L. Fritz for discussions and to DFG SPP 1459 and BMBF for support.

Note added in proof.—Recently, we became aware of a related study by J. Lux and L. Fritz [36].

[1] A. G. Rojo, J. Phys. Condens. Matter **11**, R31 (1999).
[2] P. M. Solomon, P. Price, D. Frank, and D. La Tulipe, Phys. Rev. Lett. **63**, 2508 (1989); T. J. Gramila, J. Eisenstein, A. MacDonald, L. Pfeiffer, and K. West, Phys. Rev. Lett. **66**, 1216 (1991).
[3] D. Snoke, Science **298**, 1368 (2002).
[4] M. Yamamoto, M. Stopa, Y. Tokura, Y. Hirayama, and S. Tarucha, Science **313**, 204 (2006).
[5] R. Pillarisetty, H. Noh, E. Tutuc, E. De Poortere, K. Lai, D. Tsui, and M. Shayegan, Phys. Rev. B **71**, 115307 (2005).
[6] A. S. Price, A. K. Savchenko, B. N. Narozhny, G. Allison, and D. A. Ritchie, Science **316**, 99 (2007).
[7] S. Kim, I. Jo, J. Nah, Z. Yao, S. Banerjee, and E. Tutuc, Phys. Rev. B **83**, 161401(R) (2011).
[8] A. Kamenev and Y. Oreg, Phys. Rev. B **52**, 7516 (1995).
[9] A.-P. Jauho and H. Smith, Phys. Rev. B **47**, 4420 (1993); K. Flensberg, B. Hu, A.-P. Jauho, and J. Kinaret, Phys. Rev. B **52**, 14761 (1995).
[10] S. Kim and E. Tutuc, Solid State Commun. **152**, 1283 (2012).
[11] R. V. Gorbachev *et al.*, Nat. Phys. **8**, 896 (2012).
[12] B. N. Narozhny, Phys. Rev. B **76**, 153409 (2007).
[13] W. K. Tse, Ben Yu-Kaang Hu, and S. D. Sarma, Phys. Rev. B **76**, 081401 (2007).
[14] N. M. R. Peres, J. M. B. Lopes dos Santos, and A. H. Castro Neto, Europhys. Lett. **95**, 18 001 (2011).
[15] E. H. Hwang, R. Sensarma, and S. D. Sarma, Phys. Rev. B **84**, 245441 (2011).
[16] B. N. Narozhny, M. Titov, I. Gornyi, and P. Ostrovsky, Phys. Rev. B **85**, 195421 (2012).
[17] For a detailed overview of the existing literature on the Coulomb drag in graphene see M. Carrega, T. Tudorovskiy, A. Principi, M. I. Katsnelson, and M. Polini, New J. Phys. **14**, 063033 (2012).
[18] S. M. Badalyan and F. M. Peeters, Phys. Rev. B **85**, 195444 (2012); **86**, 121405(R) (2012).
[19] B. Amorim and N. M. R. Peres, J. Phys. Condens. Matter **24**, 335602 (2012).
[20] B. Scharf and A. Matos-Abiague, Phys. Rev. B **86**, 115425 (2012).
[21] Related effect of photon drag in graphene was investigated in J. Karch *et al.*, Phys. Rev. Lett. **105**, 227402 (2010).
[22] L. Ponomarenko *et al.*, Nat. Phys. **7**, 958 (2011).
[23] A. B. Kashuba, Phys. Rev. B **78**, 085415 (2008).
[24] L. Fritz, J. Schmalian, M. Müller, and S. Sachdev, Phys. Rev. B **78**, 085416 (2008); M. Müller, J. Schmalian, and L. Fritz, Phys. Rev. Lett. **103**, 025301 (2009).
[25] M. Müller, L. Fritz, and S. Sachdev, Phys. Rev. B **78**, 115406 (2008); M. Müller, L. Fritz, S. Sachdev, J. Schmalian, V. Lebedev, and M. Feigel'man, AIP Conf. Proc. **1134**, 170 (2009); M. S. Foster and I. L. Aleiner, Phys. Rev. B **79**, 085415 (2009); D. Svintsov *et al.*, arXiv:1201.0592.
[26] See Supplemental Material at http://link.aps.org/supplemental/10.1103/PhysRevLett.110.026601 for details of the quantum kinetic equation and estimates for the third-order $\rho_D^{(3)}$ and correlated-disorder ρ_D^{corr} drag contributions.
[27] Close to the Dirac point the polarization operator is determined by T. Thus, for screened Coulomb impurities τ is effectively energy independent.
[28] M. Schütt, P. M. Ostrovsky, I. V. Gornyi, and A. D. Mirlin, Phys. Rev. B **83**, 155441 (2011).
[29] J. C. W. Song and L. S. Levitov, Phys. Rev. Lett. **109**, 236602 (2012).
[30] B. N. Narozhny, I. L. Aleiner, and A. Stern, Phys. Rev. Lett. **86**, 3610 (2001).
[31] A. Levchenko and A. Kamenev, Phys. Rev. Lett. **100**, 026805 (2008).
[32] I. V. Gornyi, A. G. Yashenkin, and D. V. Khveshchenko, Phys. Rev. Lett. **83**, 152 (1999).
[33] Y.-W. Tan, Y. Zhang, H. L. Stormer, and P. Kim, Eur. Phys. J. Special Topics **148**, 15 (2007).
[34] P. M. Ostrovsky, I. V. Gornyi, and A. D. Mirlin, Phys. Rev. B **74**, 235443 (2006); Phys. Rev. Lett. **98**, 256801 (2007); Eur. Phys. J. Special Topics **148**, 63 (2007).
[35] An alternative origin of the low-T peak is a collective state of the double-layer system which requires *strong* interaction (large α) or unreasonably low T, see M. P. Mink, H. Stoof, R. Duine, M. Polini, and G. Vignale, Phys. Rev. Lett. **108**, 186402 (2012); I. L. Aleiner, D. E. Kharzeev, and A. M. Tsvelik, Phys. Rev. B **76**, 195415 (2007); M. Yu. Kharitonov and K. B. Efetov, Phys. Rev. B **78**, 241401 (2008).
[36] J. Lux and L. Fritz, Phys. Rev. B **86**, 165446 (2012).